

Cite this: *Chem. Sci.*, 2022, 13, 2270

All publication charges for this article have been paid for by the Royal Society of Chemistry

## SuFEx-enabled, chemoselective synthesis of triflates, triflamides and triflimidates†

Bing-Yu Li, <sup>a</sup> Lauren Voets, <sup>a</sup> Ruben Van Lommel, <sup>ab</sup> Fien Hoppenbrouwers, <sup>a</sup> Mercedes Alonso, <sup>b</sup> Steven H. L. Verhelst, <sup>cd</sup> Wim M. De Borggraeve <sup>\*a</sup> and Joachim Demareel <sup>\*ac</sup>

Sulfur(vi) Fluoride Exchange (SuFEx) chemistry has emerged as a next-generation click reaction, designed to assemble functional molecules quickly and modularly. Here, we report the *ex situ* generation of trifluoromethanesulfonyl fluoride ( $\text{CF}_3\text{SO}_2\text{F}$ ) gas in a two chamber system, and its use as a new SuFEx handle to efficiently synthesize triflates and triflamides. This broadly tolerated protocol lends itself to peptide modification or to telescoping into coupling reactions. Moreover, redesigning the  $\text{S}^{\text{VI}}\text{-F}$  connector with a  $\text{S}=\text{O} \rightarrow \text{S}=\text{NR}$  replacement furnished the analogous triflimidoyl fluorides as SuFEx electrophiles, which were engaged in the synthesis of rarely reported triflimidate esters. Notably, experiments showed  $\text{H}_2\text{O}$  to be the key towards achieving chemoselective trifluoromethanesulfonation of phenols vs. amine groups, a phenomenon best explained—using *ab initio* metadynamics simulations—by a hydrogen bonded termolecular transition state for the  $\text{CF}_3\text{SO}_2\text{F}$  triflylation of amines.

Received 11th November 2021

Accepted 3rd January 2022

DOI: 10.1039/d1sc06267k

rsc.li/chemical-science

## Introduction

Recent interest in high-valent sulfur species has brought about an increasing number of  $\text{S}^{\text{VI}}\text{-F}$  bond-containing connective hubs. In the framework of Sulfur(vi)–Fluoride Exchange (SuFEx) chemistry—an umbrella term for substitution events replacing fluoride at the electrophilic sulfur center—these ‘*molecular plugins*’ allow selective and efficient installation of linkages around the  $\text{S}^{\text{VI}}$  core. Especially in the last seven years, various research groups have demonstrated the potential of SuFEx hubs such as sulfonyl fluorides ( $\text{R-SO}_2\text{F}$ ),<sup>1</sup> sulfonyl fluoride ( $\text{SO}_2\text{F}_2$ ),<sup>2</sup> thionyl tetrafluoride ( $\text{SOF}_4$ ),<sup>3</sup> ethenesulfonyl fluoride (ESF,  $\text{CH}_2=\text{CH-SO}_2\text{F}$ ),<sup>2a,4</sup> and others.<sup>5</sup> The chemoselective and straightforward nature of SuFEx chemistry has enabled a range of applications in synthesis and materials.<sup>6</sup>

A particularly intriguing aspect of SuFEx chemistry is its ability to activate oxygen nucleophiles. Various OH-containing materials of different acidities and nucleophilicities have been shown to react cleanly at the sulfur center, and subsequently

transform them into useful electrophiles for further derivatization. For example, through  $\text{SO}_2\text{F}$ -containing reagents, aliphatic alcohols have been converted into alkyl fluorides<sup>7</sup> or alkylating agents,<sup>8</sup> carboxylic acids into acyl fluorides,<sup>9</sup> and silyl ethers into sulfonate esters<sup>10</sup> (Scheme 1B). A unique role in this collection is reserved for aromatic alcohols, which in reaction with  $\text{SO}_2\text{F}_2$  selectively form the valuable aryl fluorosulfates in the presence of various other nucleophiles.<sup>2a,11</sup> By far, the most commonly employed category of O-based pseudohalides consists of aryl triflates.<sup>12</sup> Even though a number of ways to prepare aryl triflates exist,<sup>13,14,15,16,17</sup> a broadly applicable protocol that uses an inexpensive and atom-economic  $[\text{CF}_3\text{SO}_2]$  precursor in a chromatography-free and water-tolerable fashion is still missing from the toolbox.

Herein, we set out to investigate whether SuFEx chemistry can provide this general way of  $[\text{CF}_3\text{SO}_2]$  transfer onto complex organic molecules. Building on our previous work on sulfonyl fluoride,<sup>2b</sup> we propose trifluoromethanesulfonyl fluoride gas,  $\text{CF}_3\text{SO}_2\text{F}$  (b.p.  $-22^\circ\text{C}$ ), as a new electrophilic SuFEx hub, easily generated *via* two-chamber reactor technology and which reacts efficiently with phenols. Other nucleophiles such as carboxylic acids and amines reacted smoothly with the gas under dry conditions, identifying water as a key additive to obtain complete chemoselectivity for aromatic alcohols (Scheme 1C). Moreover, to shed some light on the mechanistic origins of this chemoselectivity, we relied on *ab initio* metadynamics simulations to gain fundamental insight into the key SuFEx transition state. Finally, we report a general synthesis of aryl trifluoromethanesulfonimide (triflimidate) esters: the rarely reported aza analogs of the AOTf scaffold. Triflimidoyl fluorides

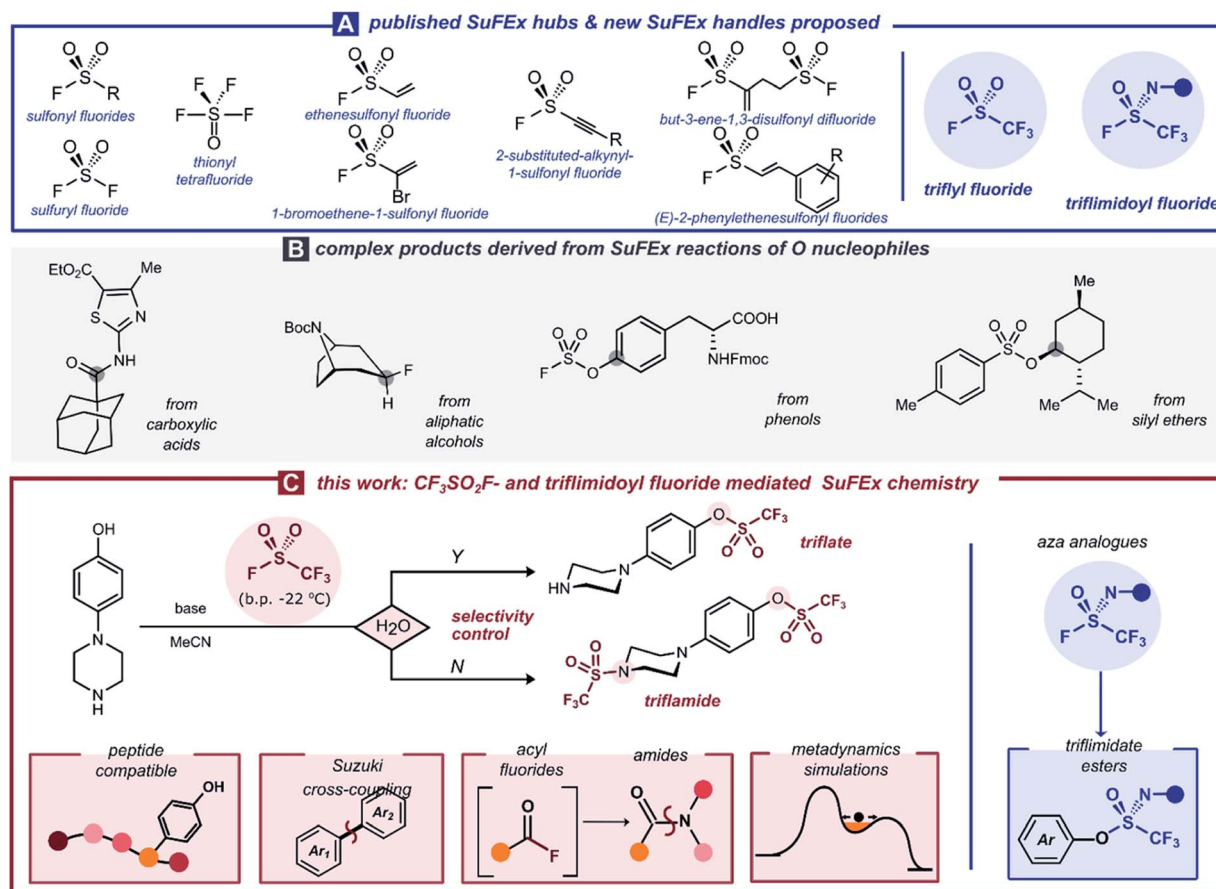
<sup>a</sup>Molecular Design and Synthesis, Department of Chemistry, KU Leuven, Celestijnenlaan 200F, Box 2404, 3001 Leuven, Belgium. E-mail: joachim.demaerel@kuleuven.be; wim.deborggraeve@kuleuven.be

<sup>b</sup>Eenheid Algemene Chemie (ALGC), Department of Chemistry, Vrije Universiteit Brussel (VUB), Pleinlaan 2, 1050 Brussels, Belgium

<sup>c</sup>Laboratory of Chemical Biology, Department of Cellular and Molecular Medicine, KU Leuven, O&N I bis, Herestraat 49, box 901, 3000 Leuven, Belgium

<sup>d</sup>Leibniz Institute for Analytical Sciences ISAS, e.V., Otto-Hahn-Str. 6b, 44227 Dortmund, Germany

† Electronic supplementary information (ESI) available. See DOI: 10.1039/d1sc06267k



**Scheme 1** (A) Selected published SuFEx hubs and new SuFEx handles proposed; (B) complex products derived from SuFEx reactions of O nucleophiles; (C) this work: CF<sub>3</sub>SO<sub>2</sub>F-mediated and *N*-substituted triflimidoxy fluoride-mediated SuFEx chemistry.

show potential as weakly electrophilic SuFEx hubs, which could have unexplored applications as covalent warheads.

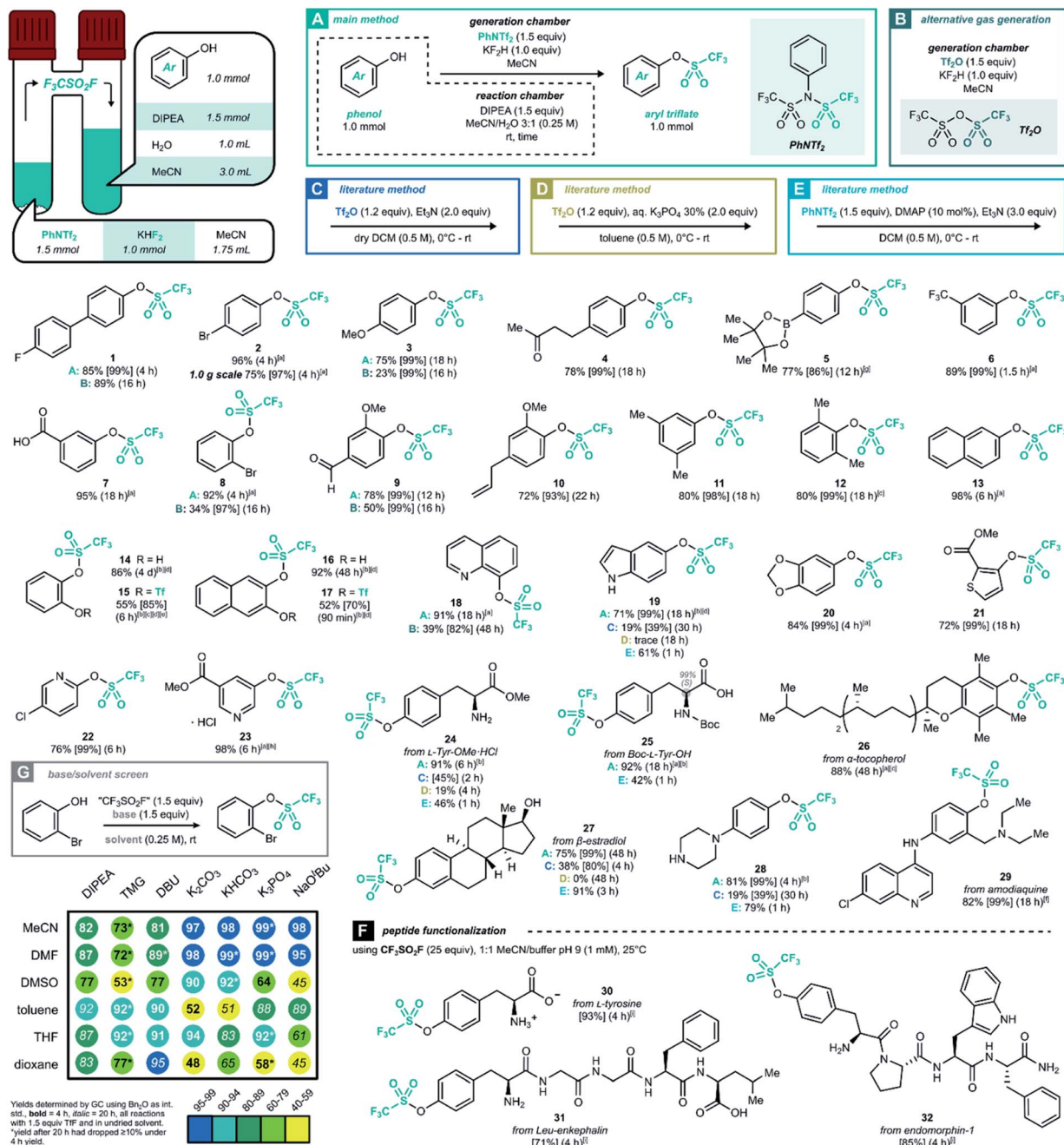
## Results and discussion

Triflyl fluoride gas was first reported in 1956 by Gramstad for the synthesis of trifluoromethanesulfonic acid derivatives.<sup>18</sup> This smallest perfluoroalkanesulfonyl fluoride is gaseous above  $-22\text{ }^{\circ}\text{C}$ , and its atmospheric chemistry is relatively innocuous.<sup>19</sup> The most relevant industrial preparation consists of the electrolytic fluorination of methanesulfonic acid or methanesulfonyl fluoride, and the resulting gas serves as the precursor to all other [CF<sub>3</sub>SO<sub>2</sub>]-containing bulk chemicals such as TfOH or Tf<sub>2</sub>O.<sup>20</sup> Other authors have prepared triflyl fluoride on a semibulk scale, by reacting CF<sub>3</sub>SO<sub>2</sub>Cl<sup>19,21</sup> or Tf<sub>2</sub>O<sup>22</sup> with a fluoride source.<sup>23</sup> Recently, Pees and co-workers have developed CF<sub>3</sub>SO<sub>2</sub><sup>18</sup>F as a carrier gas for nucleophilic [<sup>18</sup>F]-fluoride, evolving it from PhNTf<sub>2</sub> as a precursor.<sup>24</sup>

We envisaged the generation of CF<sub>3</sub>SO<sub>2</sub>F in a two-chamber reactor as the most convenient way to employ this gas safely on lab scale.<sup>25</sup> Even though a higher-MW precursor adds to the process mass intensity of this procedure, the results obtained with *ex situ* CF<sub>3</sub>SO<sub>2</sub>F gas remain true on larger scales in which case the precursor would be abandoned for direct use of gas

bottles. Inspired by the aforementioned results, we set out to develop a CF<sub>3</sub>SO<sub>2</sub>F gas generation method using PhNTf<sub>2</sub> as a bench-stable and easily handled solid precursor (for optimization, see ESI Section 3†). To our delight, the final reaction conditions allowed conversion of the model substrate 4-fluoro-4'-hydroxybiphenyl into product **1** in 85% yield after 4 hours at room temperature (Scheme 2A). With optimized conditions of method **A** in hand, a variety of readily accessible phenol derivatives was examined to further explore the scope of this methodology (Scheme 2). First, monosubstituted electron-rich and deficient phenols were successfully transformed into their corresponding triflates (**2–8**). Sterically hindered triflates **8**, **12** and **27** were also formed efficiently. Although <sup>19</sup>F NMR monitoring of catechols showed a high degree of ditriflation at the reaction onset, they nevertheless converged to the mono-triflates (**14** and **16**) after longer reaction times, most likely due to subsequent hydrolysis (see ESI Section 5.1†). With a few experimental adaptations and shorter reaction times, however, it was possible to get the less stable ditriflates **15** and **17** in a fair isolated yield. The triflation of two L-tyrosine derivatives not only offered corresponding products in excellent yields (**24** and **25**), but also without loss of enantiopurity (**25**). When it comes to naturally occurring phenols, all afforded the corresponding monotriflates in good to excellent





**Scheme 2** Synthesis of aryl triflates through *ex situ* generation of CF<sub>3</sub>SO<sub>2</sub>F gas in a two-chamber reactor. Unless stated otherwise, method A was used. Generation chamber: *N*-phenyltrifluoromethanesulfonimide (PhNTf<sub>2</sub>, 1.5 equiv.), KHF<sub>2</sub> (1.0 equiv.) and MeCN (0.86 M, 1.75 mL) at room temperature. Reaction chamber: (hetero)aryl alcohol (1.0 mmol, 1.0 equiv.), *N,N*-diisopropylethylamine (DIPEA, 1.5 equiv.) in 3.0 mL of MeCN and 1.0 mL of H<sub>2</sub>O. Reaction details see ESI Section 4.† Isolated yield after column chromatography unless stated otherwise. Between brackets is given the <sup>19</sup>F NMR yield using PhCF<sub>3</sub> as internal standard, between parentheses the reaction time. [a] Isolated yield after aqueous work-up. [b] 2.5 equiv. of DIPEA were used in the reaction chamber. [c] 3 mL MeCN was used in the reaction chamber as solvent, and the crude reaction mixture was purified on silica directly without aqueous work-up. [d] 2.5 equiv. of PhNTf<sub>2</sub> and 1.67 equivalents of KHF<sub>2</sub> were used in the generation chamber. [e] The reaction was set under Argon atmosphere. [f] Et<sub>3</sub>N (3.5 equiv.) and DMSO (0.25 M, 4.0 mL) were used in the reaction chamber. [g] The corresponding boronic acid was used as the starting material, and protected afterwards with pinacol. [h] Yield corresponds to product isolated as an HCl salt. [i] The assay yield is reported (average over two runs), defined by dividing the [M + 132] peak area by the total AUC of the HPLC-MS TIC chromatogram.

yields (**4**, **9**, **10**, **19**, **20**, **26**, **27** and **29**). In addition, three heteroaryl triflates were obtained in good to excellent yields (**21**, **22** and **23**). It is worth pointing out that in many cases, the two-

chamber reactor method afforded the triflates in sufficiently pure form after extractive work-up, without the need for column chromatography.



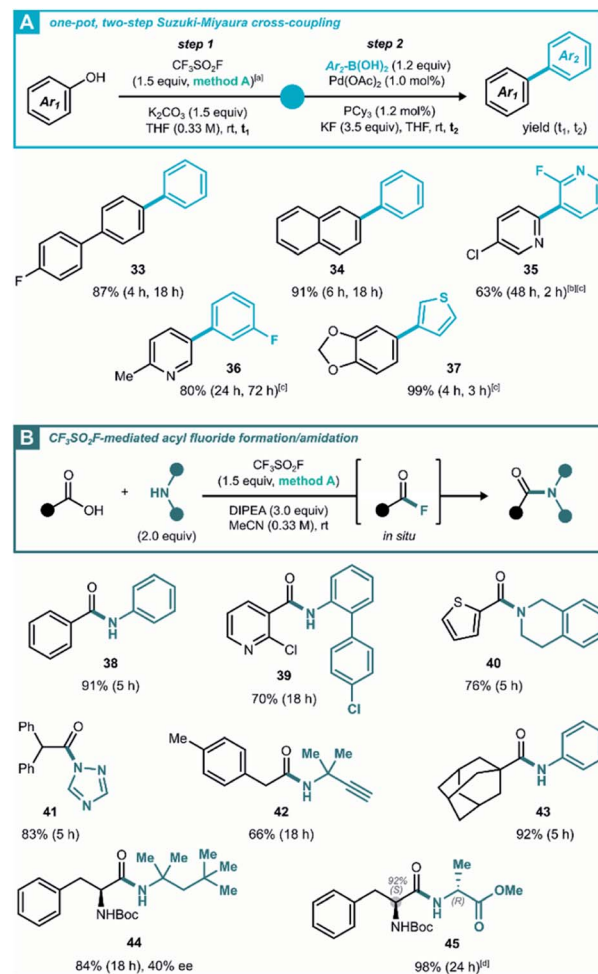


In parallel to this method, a different set of conditions was developed using  $\text{TF}_2\text{O}$  as the gas precursor,<sup>22</sup> a less expensive and commonly available chemical (method B). Even though good results were obtained for simple phenols (**1**), the unpleasant nature of this fuming and sensitive liquid, and the reduced yields for more complex phenols (**3**, **8**, **9** and **18**) make this method less ideal. Next, in order to further assess the validity of  $\text{CF}_3\text{SO}_2\text{F}$  as a triflating agent, our method was benchmarked against other known triflation methods (for details, see ESI Section 4.1.3†). Four representative phenols were treated according to three literature triflation protocols: adding  $\text{TF}_2\text{O}$  to a solution of phenol and organic base (method C);<sup>26</sup> adding  $\text{TF}_2\text{O}$  under Frantz' aqueous conditions (method D)<sup>27</sup> and using the  $\text{PhNTf}_2$  reagent directly (method E).<sup>28</sup> Even though the gas-free methods required a shorter reaction time, the corresponding triflates were almost universally obtained in lower yield than with  $\text{CF}_3\text{SO}_2\text{F}$ . Not only did the literature methods require more careful temperature control or moisture exclusion, also the chemoselectivity was usually inferior when the phenol starting materials contained indoles (**19**), aliphatic amines (**24** and **28**), carboxylic acids (**25**) or aliphatic alcohols (**27**). Moreover, amine **28** did not show any trace of sulfonamide formation, even with 2.5 equivalents of gas (see ESI Section 5.2.1†). To sum up, our  $\text{CF}_3\text{SO}_2\text{F}$  gas-based two-chamber system allowed triflation to proceed in a stable, productive and chemoselective fashion.

During the development of this work, it was observed that the aryl triflate synthesis was relatively insensitive towards the choice of solvent or base. To further showcase the versatility of this SuFEx reaction, a series of solvent–base combinations was explored (Scheme 2G). While maintaining the original gas generation using  $\text{PhNTf}_2$ , a set of 7 bases (organic and inorganic) was screened against a set of 6 commonly used reaction solvents. In almost all cases, the reactions had reached >50% conversion after 20 h, and the majority even >80% under unoptimized conditions. While some of the stronger bases were more prone to cause product degradation, nevertheless this broad compatibility enables a subsequent reaction step without intermediate  $\text{ArOTf}$  isolation.

Given the variety of allowed solvent/base combinations, we wondered whether the triflation method can reach further synthetic utility in a one-pot Suzuki–Miyaura cross-coupling reaction. Based on a literature protocol,<sup>29</sup> we found that the (hetero)aryl triflates underwent efficient cross-coupling by transferring the reaction mixture to a vial with the (hetero)aryl boronic acid, palladium(II) acetate and tricyclohexylphosphine (Scheme 3A). With this protocol, biaryls **33–37** were synthesized under mild conditions with good to near-quantitative isolated yield over two steps. The more challenging bipyridine **35** was prepared in a 1,4-dioxane/ $\text{H}_2\text{O}$  mixture in 63% yield, which was higher than the 42% yield reported in literature.<sup>30</sup> In addition, this Suzuki cross-coupling afforded 2-methyl-5-(3-fluorophenyl)pyridine **36**, the pharmacophore of vorapaxar<sup>31</sup> in 80% yield without purifying the intermediate triflate.

Another class of oxygen nucleophiles that was subjected to  $\text{CF}_3\text{SO}_2\text{F}$ -enabled post-transformations, consists of carboxylic acids. In line with Moses<sup>9c</sup> and Qin's<sup>9b</sup> work on SuFEx-mediated



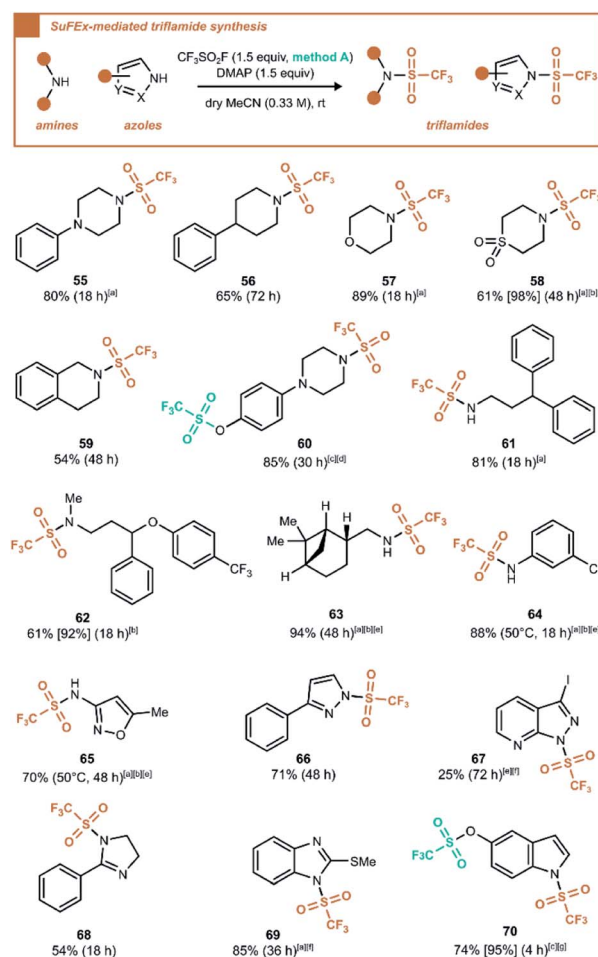
**Scheme 3** One-pot reactions enabled by  $\text{CF}_3\text{SO}_2\text{F}$  gas generation. (A) One-pot, two-step method of aryl triflate generation followed by Suzuki–Miyaura cross-coupling. (B) Amide synthesis with *in situ* generated acyl fluorides. The yield corresponds in all cases to the isolated yield after column chromatography without isolation of the intermediates; the enantiomeric excess (ee) was determined by HPLC analysis. [a] DMF was used in the generation chamber instead of MeCN for volatility reasons. [b]  $\text{NaHCO}_3$  was used as the only base (1.5 + 2.2 equiv. in step 1 and 2, resp.), with 1,4-dioxane/ $\text{H}_2\text{O}$  5 : 1 as the solvent, step 2 was heated to 80 °C. [c]  $\text{Pd(OAc)}_2$  (2.0 mol%) and  $\text{PCy}_3$  (2.4 mol%) were used. [d] The product was isolated as a 92 : 8 mixture of diastereoisomers, which was detected by  $^1\text{H}$  NMR.

carboxylic acid activation, we aimed to develop a new method based on generating acyl fluoride intermediates *via*  $\text{CF}_3\text{SO}_2\text{F}$  gas (Scheme 3B). Without isolating the acyl fluorides, they were reacted immediately to build amides with various degrees of steric congestion. Where the biphasic conditions developed in Scheme 2A left carboxylic acids untouched (products **7** and **25**), simply shifting to a pure organic solvent led to smooth deoxo-fluorination. To explore the substrate scope and functional group tolerance of the amidation process, a variety of aromatic and aliphatic carboxylic acids were examined for coupling with different kinds of amines, including anilines, primary and secondary alkylamines and azoles. All coupling reactions proceeded in fair to excellent yields (Scheme 3, **38–44**). This work

l-tyrosine methyl ester (**53**), raspberry ketone (**54**), as well as sterically hindered 2-bromophenol (**51**) and thiophen-2-ol (**48**) were all well tolerated (Scheme 4).

After the transformation of various oxygen nucleophiles into reactive handles with  $\text{CF}_3\text{SO}_2\text{F}$ , we also wanted to investigate nitrogen nucleophiles. To this end, a range of aliphatic amines, anilines and azoles was engaged in a triflylating reaction to form the trifluoromethanesulfonamides (triflamides) (Scheme 5). Based on a literature SuFEx reaction between  $\text{SO}_2\text{F}_2$  and secondary amines,<sup>2a</sup> we selected DMAP as a stoichiometric base, although we found later that  $\text{Et}_3\text{N}$  furnishes the same products in equal reaction times and yields with the dry MeCN served as the solvent.

Under these conditions, secondary amines (**55–60**, **62**) reacted efficiently to form the tertiary sulfonamides. Also, primary amines (**61**, **63–65**) were suitable reaction partners to form N-



**Scheme 5** Synthesis of triflamides by reaction of  $\text{CF}_3\text{SO}_2\text{F}$  with amines and azoles. Reaction was carried out on 1.0 mmol scale and reported yields are after column chromatography unless noted otherwise. Between brackets is given the  $^{19}\text{F}$  NMR yield using  $\text{PhCF}_3$  as internal standard, between parentheses the reaction time. [a] Isolated yield of pure material after aqueous work-up. [b] 3.0 equiv. of base was used. [c] 2.5 equiv. of  $\text{CF}_3\text{SO}_2\text{F}$  gas was used. [d] 3.5 equiv. of base was used. [e] 2.0 equiv. of  $\text{CF}_3\text{SO}_2\text{F}$  was generated. [f]  $\text{K}_2\text{CO}_3$  was used as the base. [g] 2.5 equiv. of base was used.

**Scheme 4** SuFEx-enabled synthesis of aryl triflimidate esters from triflimidoaryl fluorides. Reactions were carried out at a 0.2 mmol scale. [a] 1.1 equiv. of ArOH was used. [b] 1.2 equiv. of ArOH used, reaction time was 3 h. [c] Reaction was carried out at a 2.0 mmol scale.

monosubstituted triflamides, an interesting contrast with monosubstituted sulfamoyl fluorides, which cannot be formed under basic conditions.<sup>2a</sup> Finally, except for a few unsuccessful substrates (see ESI Section 7.7†), various *N*-triflyl heterocycles were prepared in the same manner in fair to good yields (66–70). It is worth noting that the *N,O*-bis(trifluoromethanesulfonyl) compound **60** was formed in high yield using 2.5 equivalents of the generated gas. This stands in contrast to the reaction leading to **28**, where no trace of *N*-triflyl product was observed. The same discrepancy was observed for **70** vs. **19**. It was also verified that *N*-triflyl compounds **60** and **70** were not hydrolysed by water (see ESI Section 5.3 and 5.4†). Since the only difference between these reaction conditions is the presence or absence of water, it seems that water influences the mechanism in such a way that it plays a decisive role in the reaction outcome. Ultimately, a direct reactivity comparison of phenol and amine groups in compound **60** was evaluated using only 1.0 equiv. of CF<sub>3</sub>SO<sub>2</sub>F gas. Regardless of choice of base, the product mixtures resulting from trifluoromethanesulfonation in anhydrous MeCN invariably lacked N-SO<sub>2</sub>CF<sub>3</sub> monotriflylated product, indicating highest reactivity for the phenol group (see ESI Section 5.2.2†).

Having established a robust procedure for installing a triflyl group through our CF<sub>3</sub>SO<sub>2</sub>F SuFEx hub, we turned towards the mechanism of this reaction. More specifically, we investigated the base-mediated triflylation of secondary amines, aiming to elucidate the reaction pathway and the specific role of the base. As a result, we hope to shed light on the observed chemoselectivity, by comparing our simulations for secondary amines with the better-studied mechanism of phenol SuFEx reactions.<sup>35,37</sup> To achieve this goal, we use *ab initio* metadynamics (AIMtD) to retrieve the mechanism as well as quantify the associated activation barriers.<sup>38</sup> In contrast to static DFT computations, AIMtD usually includes all molecules in the simulation box, meaning explicit interactions between reactants and additives or solvents are accurately modelled, with the trade-off of a significant increase in computational workload (for theoretical background, see ESI Section 8.1†). We, among others, have previously shown the ability of AIMtD to elucidate reaction mechanisms, quantify reaction barriers and unveil solvation effects.<sup>39</sup> Here, piperidine served as a case study for the computationally modelled CF<sub>3</sub>SO<sub>2</sub>F triflylation reaction (Fig. 1A). In parallel, a series of experimental studies was performed, to complement the *in silico* findings (Fig. 1B).<sup>40</sup> Initially, three different systems were considered. A single CF<sub>3</sub>SO<sub>2</sub>F and one piperidine molecule were placed in the simulation box together with explicit acetonitrile (I), or with DMAP (II) or Et<sub>3</sub>N (III) included as a base (Fig. 1A). All simulations in this study followed the Born–Oppenheimer molecular dynamics scheme at the DFT level of theory, with the GGA PBE functional and DZVP-MOLOPT-GTH plane wave basis set.<sup>41</sup> Additionally, the description of long-range dispersion interactions was improved by Grimme's D3 dispersion correction.<sup>42</sup> The CP2K code (version 6.1) was used together with the Quickstep implementation (for full computational details see ESI Section 8.1†).<sup>43</sup>

From analysing the trajectory obtained for the non-activated CF<sub>3</sub>SO<sub>2</sub>F-triflylation of piperidine (I), a concerted bimolecular

reaction mechanism was observed, akin to an S<sub>N</sub>2-type pathway (see ESI Movie†). Indeed, bond length analysis shows a simultaneous S–F bond breaking and S–N<sub>pip</sub> bond formation (see ESI Section 8.1†) and the free energy surface displays a reactant and product phase, without an additional intermediate basin (Fig. 1A, I). Notably, without a base, the piperidine nucleophile attacks the sulfur-center from the frontside, which for most S<sub>N</sub>2 reactions would be less favourable compared to the corresponding backside pathway.<sup>44</sup> Herein, frontside attack allows F<sup>–</sup> to directly scavenge the amine hydrogen of piperidine.

While this mechanism coincides with the findings of Luy and Tonner, the AIMtD simulations result in a Helmholtz free energy of activation ( $\Delta F^\ddagger$ ) of  $29 \pm 4$  kcal mol<sup>–1</sup>, which exceeds a barrier that can readily be crossed at ambient conditions.<sup>37</sup> As the non-activated triflylation of **55** yielded 49% of product at room temperature after 18 hours (Fig. 1B, entry 1), the obtained high activation barrier raises questions on the validity of this mechanism. When adding a base such as DMAP (A, II) or Et<sub>3</sub>N (A, III) to the simulation box, a significantly reduced  $\Delta F^\ddagger$  is observed ( $13 \pm 1$  kcal mol<sup>–1</sup> and  $22.1 \pm 0.05$  kcal mol<sup>–1</sup>, respectively, Fig. 1A). These activation barriers are reasonable, given the high experimental yields obtained for the base-mediated triflylation of **55** (entries 2–3). Mechanistically, the reaction occurs concertedly when DMAP or Et<sub>3</sub>N are used, similar to the non-activated CF<sub>3</sub>SO<sub>2</sub>F-triflylation of piperidine (see ESI Section 8.1 and Movie†). Moreover, the trajectory indicates that the base forms a Lewis adduct with piperidine through a hydrogen bond, enhancing the nucleophilicity of N<sub>pip</sub>. Collectively, these observations indicate that the transition state has a termolecular nature, meaning the reaction follows an S<sub>N</sub>3-type pathway. While initially these findings might seem surprising, such S<sub>N</sub>3 pathways have previously been proposed as mechanisms for substitution reactions on sulfonyl substrates.<sup>45</sup> Moreover, when the reaction is activated by DMAP or Et<sub>3</sub>N, backside attack of the nucleophile is preferred.

Another intriguing observation was the difference between  $\Delta F^\ddagger$  of the DMAP and Et<sub>3</sub>N activated triflylation. One would expect that a stronger base would activate the nucleophile more efficiently and thus further decrease the activation barrier. Nevertheless, our AIMtD simulations resulted in a value for  $\Delta F^\ddagger$  of  $13 \pm 1$  kcal mol<sup>–1</sup> and  $21.9 \pm 0.5$  kcal mol<sup>–1</sup> for DMAP and Et<sub>3</sub>N, respectively. In other words, the activating role of Et<sub>3</sub>N is significantly less effective compared to DMAP, notwithstanding Et<sub>3</sub>N is the stronger base. To further study the differences between the DMAP-mediated and Et<sub>3</sub>N-mediated triflylation of piperidine, NCI analyses were performed on their transition states (for theoretical background, see ESI Section 8.2†).<sup>46</sup> Remarkably, the 3D NCI isosurface of the DMAP-mediated transition state and bond length analysis reveals an attractive non-classical CH<sup>⋯</sup>O hydrogen bond connecting DMAP with CF<sub>3</sub>SO<sub>2</sub>F (Fig. 1C, purple arrow and ESI Section 8.1†). The synergy between this CH<sup>⋯</sup>O hydrogen bond and Lewis adduct formation between DMAP and piperidine favourably align both reactants in the transition state. Furthermore, the isosurface of the Et<sub>3</sub>N-mediated transition state is characterized by larger repulsive (red) surfaces compared to the DMAP-mediated transition state, especially between Et<sub>3</sub>N and CF<sub>3</sub>SO<sub>2</sub>F. From the number of peaks





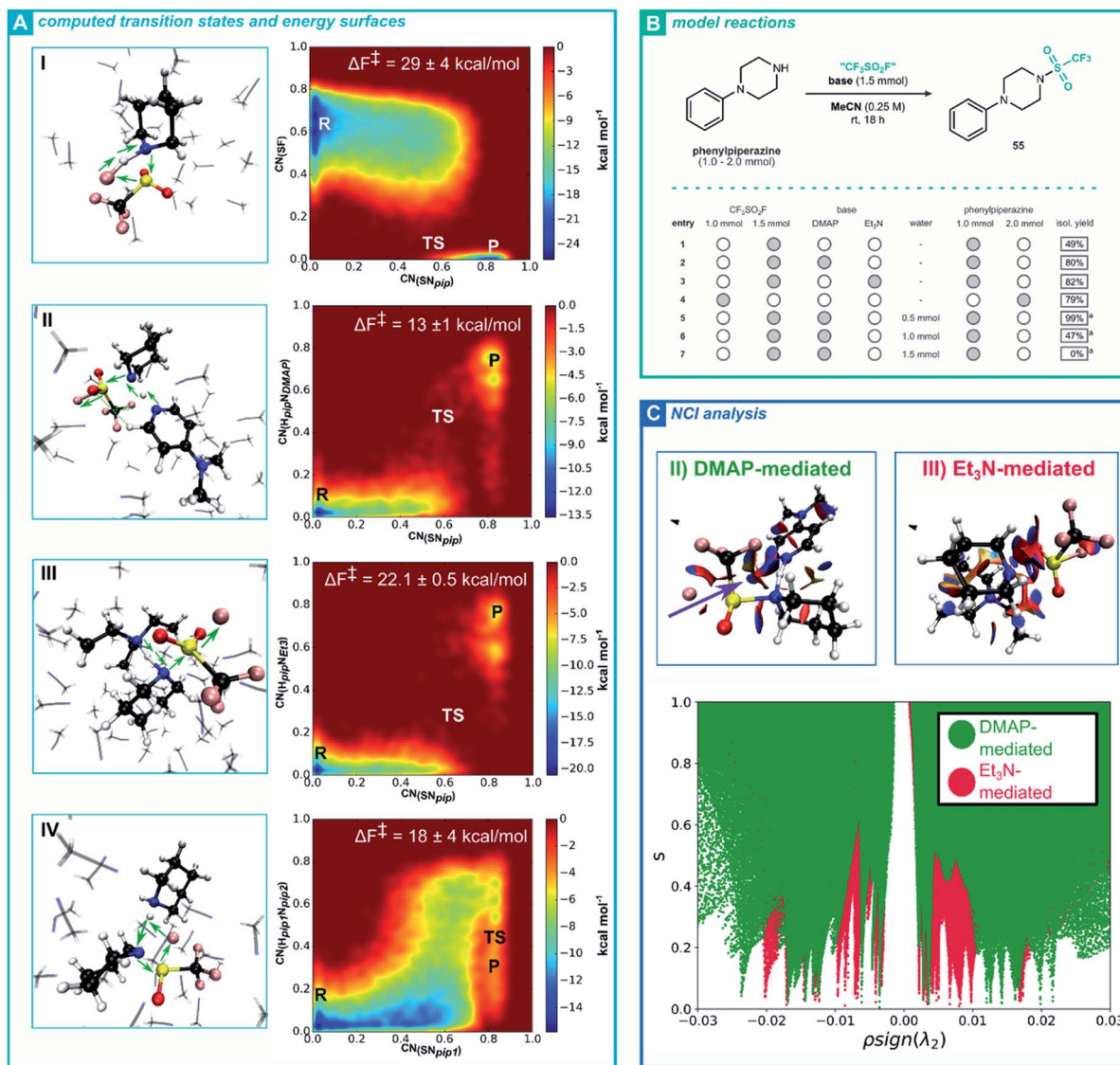
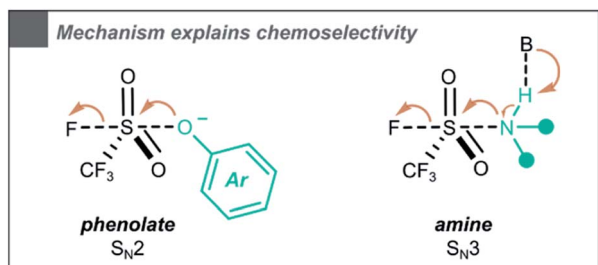


**Fig. 1** (A) Transition states obtained through metadynamics simulations for: (I) the non-activated  $\text{CF}_3\text{SO}_2\text{F}$ -triflylation of piperidine in acetonitrile, (II) the DMAP-activated  $\text{CF}_3\text{SO}_2\text{F}$ -triflylation of piperidine in acetonitrile, (III) the  $\text{Et}_3\text{N}$ -activated  $\text{CF}_3\text{SO}_2\text{F}$ -triflylation of piperidine in acetonitrile and (IV) the non-activated  $\text{CF}_3\text{SO}_2\text{F}$ -triflylation of piperidine in acetonitrile including two molecules of piperidine. In all cases, electron displacement is schematically illustrated using green arrows. During the simulations, Gaussian shaped potentials were placed along two coordination numbers, resulting in a free energy surface and Helmholtz free energy of activation ( $\Delta F^\ddagger$ ). Simulations were performed in triplicate. (B) Triflylation of phenylpiperazine as model reaction varying the base, solvent and relative amounts of substrate and  $\text{CF}_3\text{SO}_2\text{F}$ . Isolated yields are provided unless stated otherwise. [a]  $^{19}\text{F}$  NMR yield relative to int. std. after 72 h reaction time. (C) NCI analyses were performed on the transition states of the DMAP-mediated  $\text{CF}_3\text{SO}_2\text{F}$  triflylation (II, green) and  $\text{Et}_3\text{N}$ -mediated  $\text{CF}_3\text{SO}_2\text{F}$  triflylation (III, red). Analyses were performed in absence of the solvent to focus on the noncovalent interactions present in and between the reactive species. Top; 3D NCI isosurfaces ( $s = 0.5$ ) visualized for both reactive systems. An RGB-scale is used to differentiate between repulsive (red) and attractive (green) interactions, set from  $-0.005$  a.u. to  $0.005$  a.u. For the DMAP-mediated triflylation, a non-classical  $\text{CH}\cdots\text{O}$  hydrogen bond is observed as an attractive blue surface, which connects DMAP with  $\text{CF}_3\text{SO}_2\text{F}$  (purple arrow). Bottom; an overlay plot of  $s$  against  $\rho \text{sign}(\lambda_2)$  is presented for both NCI analyses.

present in the plot of  $s$  against  $\rho \text{sign}(\lambda_2)$ , it can also be inferred that the  $\text{Et}_3\text{N}$ -mediated transition state contains considerably more noncovalent interactions (Fig. 1C). Based on these results, we believe that the activating role of the base in the  $\text{CF}_3\text{SO}_2\text{F}$ -triflylation of piperidine transcends beyond deprotonation of the amine. Clearly, intricate non-covalent interactions such as hydrogen bonding or steric repulsion due to the bulkiness of all reactants involved play an important role in the stability of the termolecular transition state.

After establishing plausible reaction pathways for the activated triflylation of piperidine, we reconsidered the mechanism for the non-activated reaction (A, I). We reasoned that, besides acting as the nucleophile, a second equivalent of piperidine could activate the reaction, similar to an added base. Such a mechanistic picture would also coincide with the non-activating triflylation of 55 yielding 49% of product (Fig. 1B entry 1). Indeed, a maximum of 50% would be expected when the substrate acts as its own base. To our delight, we obtained





Scheme 6 The  $\text{CF}_3\text{SO}_2\text{F}$  triflylation of phenols (phenolate as reactive species) and amines occurs through different pathways.

an energetically more reasonable mechanism for the non-activated triflylation of piperidine when a second piperidine molecule was added to the simulation box, resulting in a  $\Delta F^\ddagger$  of  $18 \pm 4 \text{ kcal mol}^{-1}$  (A, IV). In this mechanism, a second equivalent of piperidine forms a Lewis adduct with the piperidine nucleophile and a termolecular transition state is observed. A notable difference with the activated pathways (A, II and III), is that herein substitution preferably proceeds through frontside attack of the nucleophile. To further strengthen our hypothesis, the relative amount of phenylpiperazine with respect to  $\text{CF}_3\text{SO}_2\text{F}$  was increased (2 : 1 ratio). As expected, the experimental yield of the reaction increased to 79% (entry 4), suggesting that indeed a second equivalent of piperidine plays an active part in the reaction. Intriguingly, when the water content is gradually increased, as little as 1.5 equivalent shuts down the reaction completely (entries 5–7).

Based on these mechanistic insights, we propose an explanation for the observed chemoselectivity when comparing the triflylation of amines and phenols. When performing the reaction in  $\text{MeCN} : \text{H}_2\text{O}$  (3 : 1), phenols are selectively triflylated, while amines remain unaffected (compounds **19** and **28**). On the other hand, in dry  $\text{MeCN}$  (0.33 M), both phenols and amines are converted (compounds **60** and **70**). We believe that the influence of  $\text{H}_2\text{O}$  on chemoselectivity can be explained through the difference in mechanism. A trialkylamine ( $\text{p}K_{\text{aH}} \sim 11$ ) will partially deprotonate the phenol ( $\text{p}K_{\text{aH}} \sim 10$ ) towards the phenolate, which is likely to undergo triflylation *via* a bimolecular  $\text{S}_{\text{N}}2$  type mechanism, as shown by Zuilhof and co-workers.<sup>35</sup> In contrast, our simulations showed that under the same conditions, amines would undergo an  $\text{S}_{\text{N}}3$  type mechanism, in which a hydrogen bond driven Lewis adduct between the nucleophile and the base is formed (Scheme 6). We assume  $\text{H}_2\text{O}$  to disrupt these essential hydrogen bonds, explaining why the reaction in  $\text{MeCN} : \text{H}_2\text{O}$  is selective towards phenols, while in dry  $\text{MeCN}$  both phenols and amines showcase a high reactivity towards triflylation.

## Conclusions

To summarize, we designed a two-chamber procedure for the safe and efficient *ex situ* handling of triflyl fluoride gas ( $\text{CF}_3\text{SO}_2\text{F}$ ) as a new type of SuFEx connector. Herewith, a diverse library of triflates and triflamides was built straightforwardly, often without the need for further purification. Comparing with literature triflation methods,  $\text{CF}_3\text{SO}_2\text{F}$  consistently furnished higher

yields and selectivities. A particularly interesting finding was the lack of reactivity of carboxylic acids and amines in the presence of water, allowing a completely chemoselective triflylation of phenolic nucleophiles. In a more in-depth study of this phenomenon, *ab initio* metadynamics (AIMtD) simulations offered insight into the reactivity of the  $\text{CF}_3\text{SO}_2\text{F}$  triflylation with secondary amine nucleophiles. In contrast to phenolates reacting in a bimolecular fashion, the simulations for amines suggested a formal  $\text{S}_{\text{N}}3$  mechanism with a termolecular transition state that relies on hydrogen bond formation between base and nucleophile. Due to the absence of such H-bonds in aqueous media, we believe this mechanism explains the observed difference in reaction outcome. The formation of aryl triflates proved amenable to peptide functionalization and reaction telescoping into one-pot Suzuki–Miyaura cross-coupling. In addition, the sulfonylation chemistry developed for triflyl fluoride  $\text{CF}_3\text{SO}_2\text{F}$  was found to be fully translatable to triflimidoyle fluorides  $\text{CF}_3\text{-SO}(\text{NR})\text{F}$ . These aza-analogous SuFEx hubs provided an efficient route to aryl triflimidate esters, a barely reported class of compounds with three-dimensional, potentially chiral character and unknown biological properties. Overall, we believe that the *ex situ* gas generation method will lead to increased use of  $\text{CF}_3\text{SO}_2\text{F}$  in chemoselective, lab-scale synthesis of valuable aryl triflates and triflamides. Also, process chemistry may benefit from the clean reaction profiles demonstrated here, when using gaseous  $\text{CF}_3\text{SO}_2\text{F}$  directly as a low-MW progenitor to current standard  $\text{Tf}_2\text{O}$ . Ultimately, we believe the insights derived from high-quality *ab initio* calculations form the next step in understanding the fundamental interactions during  $\text{S}^{\text{VI}}\text{-F}$  chemistry, and provide a better-informed basis for future applications.

## Data availability

All experimental data, procedures for data analysis and pertinent data sets are provided in the ESI.†

## Author contributions

J. D., W. M. D. B., S. H. L. V., and B.-Y. L conceived the formulation and evolution of overarching research goals and aims. B.-Y. L, L. V, F. H and J. D. performed the experiments. R. V. L and M. A performed computational calculations. J. D., B.-Y. L and R. V. L wrote the original draft. All the authors discussed the results and contributed to edit the manuscript.

## Conflicts of interest

There are no conflicts to declare.

## Acknowledgements

We are grateful to Bart Van Huffel and Luc Baudemprez for the assistance with NMR measurements and to Bart Van Huffel for the elemental analysis. We kindly acknowledge Marcus Frings for HPLC analyses. B.-Y. L thanks the CSC (Chinese Scholarship Council) for her fellowship received. J. D., L. V, R. V. L, M. A and W. M. D. B. thank FWO Vlaanderen (Research Foundation –





Flanders) for fellowships and grants received (12ZL820N, 1SA1121N, 1185221N, 12F4416N, G0D6221N). M. A. thanks Vrije Universiteit Brussel (VUB) for financial support. W. M. D. B. thanks KU Leuven for financial support via Project DOA/2020/013. S. H. L. V. acknowledges financial support from the Ministerium für Kultur und Wissenschaft des Landes Nordrhein-Westfalen, the Regierende Bürgermeister von Berlin-inkl. Wissenschaft und Forschung, and the Bundesministerium für Bildung und Forschung. Mass spectrometry was made possible by the support of the Hercules Foundation of the Flemish Government (grant 20100225-7). Tier2 computational resources and services were provided by the Shared ICT Services Centre funded by the VUB, the Flemish Supercomputer Center (VSC) and FWO. Tier1 computational resources and services that were used in this work were provided by the VSC, funded by the FWO and the Flemish Government-department EWI.

## Notes and references

- (a) J. C. Brendel, L. Martin, J. Zhang and S. Perrier, *Polym. Chem.*, 2017, **8**, 7475–7485; (b) H. Wang, F. Zhou, G. Ren, Q. Zheng, H. Chen, B. Gao, L. Klivansky, Y. Liu, B. Wu, Q. Xu, J. Lu, K. B. Sharpless and P. Wu, *Angew. Chem., Int. Ed.*, 2017, **56**, 11203–11208; (c) T. Hmissa, X. Zhang, N. R. Dhumal, G. J. McManus, X. Zhou, H. B. Nulwala and A. Mirjafari, *Angew. Chem., Int. Ed.*, 2018, **57**, 16005–16009; (d) S. Park, H. Song, N. Ko, C. Kim, K. Kim and E. Lee, *ACS Appl. Mater. Interfaces*, 2018, **10**, 33785–33789; (e) B. Yang, H. Wu, P. D. Schnier, Y. Liu, J. Liu, N. Wang, W. F. DeGrado and L. Wang, *Proc. Natl. Acad. Sci. U. S. A.*, 2018, **115**, 11162–11167; (f) G. Laudadio, A. d. A. Bartolomeu, L. M. H. M. Verwijlen, Y. Cao, K. T. de Oliveira and T. Noël, *J. Am. Chem. Soc.*, 2019, **141**, 11832–11836; (g) W. Liu, S. Zhang, S. Liu, Z. Wu and H. Chen, *Macromol. Rapid Commun.*, 2019, **40**, 1900310.
- (a) J. Dong, L. Krasnova, M. G. Finn and K. B. Sharpless, *Angew. Chem., Int. Ed.*, 2014, **53**, 9430–9448; (b) C. Veryser, J. Demaerel, V. Bieliūnas, P. Gilles and W. M. De Borggraeve, *Org. Lett.*, 2017, **19**, 5244–5247; (c) J. D. Randall, D. J. Eyckens, F. Stojcevski, P. S. Francis, E. H. Doeven, A. J. Barlow, A. S. Barrow, C. L. Arnold, J. E. Moses and L. C. Henderson, *ChemPhysChem*, 2018, **19**, 3176–3181; (d) J. Kwon and B. M. Kim, *Org. Lett.*, 2018, **21**, 428–433; (e) C. Lee, N. D. Ball and G. Sammis, *Chem. Commun.*, 2019, **55**, 14753–14756; (f) Q. Zheng, J. L. Woehl, S. Kitamura, D. Santos-Martins, C. J. Smedley, G. Li, S. Forli, J. E. Moses, D. W. Wolan and K. B. Sharpless, *Proc. Natl. Acad. Sci. U.S.A.*, 2019, **116**, 201909972.
- (a) S. Li, P. Wu, J. E. Moses and K. B. Sharpless, *Angew. Chem., Int. Ed.*, 2017, **56**, 2903–2908; (b) B. Gao, S. Li, P. Wu, J. E. Moses and K. B. Sharpless, *Angew. Chem., Int. Ed.*, 2018, **57**, 1939–1943.
- (a) Q. Chen, P. Mayer and H. Mayr, *Angew. Chem., Int. Ed.*, 2016, **55**, 12664–12667; (b) Q. Zheng, J. Dong and K. B. Sharpless, *J. Org. Chem.*, 2016, **81**, 11360–11362; (c) H. L. Qin, Q. Zheng, G. A. Bare, P. Wu and K. B. Sharpless, *Angew. Chem., Int. Ed.*, 2016, **55**, 14155–14158; (d) J. Leng and H.-L. Qin, *Chem. Commun.*, 2018, **54**, 4477–4480; (e) J. Chen, B. Q. Huang, Z. Q. Wang, X. J. Zhang and M. Yan, *Org. Lett.*, 2019, **21**, 9742–9746; (f) Y.-P. Meng, S.-M. Wang, W.-Y. Fang, Z.-Z. Xie, J. Leng, H. Alsulami and H.-L. Qin, *Synthesis*, 2020, **52**, 673–687.
- (a) C. J. Smedley, M.-C. Giel, A. Molino, A. S. Barrow, D. J. D. Wilson and J. E. Moses, *Chem. Commun.*, 2018, **54**, 6020–6023; (b) B. Moku, W.-Y. Fang, J. Leng, L. Li, G.-F. Zha, K. P. Rakesh and H.-L. Qin, *iScience*, 2019, **21**, 695–705; (c) H. Zhou, P. Mukherjee, R. Liu, E. Evrard, D. Wang, J. M. Humphrey, T. W. Butler, L. R. Hoth, J. B. Sperry, S. K. Sakata, C. J. Helal and C. W. am Ende, *Org. Lett.*, 2018, **20**, 812–815; (d) M. F. Khumalo, E. D. Akpan, P. K. Chinthakindi, E. M. Brasil, K. K. Rajbongshi, M. M. Makatini, T. Govender, H. G. Kruger, T. Naicker and P. I. Arvidsson, *RSC Adv.*, 2018, **8**, 37503–37507.
- (a) T. A. Fattah, A. Saeed and F. Albericio, *J. Fluorine Chem.*, 2018, **213**, 87–112; (b) A. S. Barrow, C. J. Smedley, Q. Zheng, S. Li, J. Dong and J. E. Moses, *Chem. Soc. Rev.*, 2019, **48**, 4731–4758.
- (a) H. Vorbrüggen, *Synthesis*, 2008, 1165–1174, DOI: 10.1055/s-2008-1067006; (b) M. K. Nielsen, D. T. Ahneman, O. Riera and A. G. Doyle, *J. Am. Chem. Soc.*, 2018, **140**, 5004–5008; (c) M. K. Nielsen, C. R. Ugaz, W. Li and A. G. Doyle, *J. Am. Chem. Soc.*, 2015, **137**, 9571–9574.
- (a) M. Epifanov, J. Y. Mo, R. Dubois, H. Yu and G. M. Sammis, *J. Org. Chem.*, 2021, **86**, 3768–3777; (b) J. Y. Mo, M. Epifanov, J. W. Hodgson, R. Dubois and G. M. Sammis, *Chem. –Eur. J.*, 2020, **26**, 4958–4962; (c) P. J. Foth, F. Gu, T. G. Bolduc, S. S. Kanani and G. Sammis, *Chem. Sci.*, 2019, **10**, 10331–10335; (d) M. Epifanov, P. J. Foth, F. Gu, C. Barrillon, S. S. Kanani, C. S. Higman, J. E. Hein and G. M. Sammis, *J. Am. Chem. Soc.*, 2018, **140**, 16464–16468; (e) C. Zhao, G.-F. Zha, W.-Y. Fang, N. S. Alharbi and H.-L. Qin, *Tetrahedron*, 2019, **75**, 4648–4656.
- (a) P. J. Foth, T. C. Malig, H. Yu, T. G. Bolduc, J. E. Hein and G. M. Sammis, *Org. Lett.*, 2020, **22**, 6682–6686; (b) S.-M. Wang, C. Zhao, X. Zhang and H.-L. Qin, *Org. Biomol. Chem.*, 2019, **17**, 4087–4101; (c) C. J. Smedley, A. S. Barrow, C. Spiteri, M.-C. Giel, P. Sharma and J. E. Moses, *Chem. –Eur. J.*, 2017, **23**, 9990–9995.
- V. Gembus, F. Marsais and V. Levacher, *Synlett*, 2008, 1463–1466, DOI: 10.1055/s-2008-1078407.
- A. Ishii, T. Ishimaru, T. Yamazaki and M. Yasumoto, Process for Producing Fluorosulfuric Acid Aromatic-ring Esters, *US Pat.*, 9040745B2, 2015.
- A concise literature discussion can be found in ESI Section 15.†
- Examples using triflic anhydride as a [Tf] source: A. G. Martínez, L. R. Subramanian, M. Hanack, S. J. Williams and S. Régnier, *Journal*, 2016, 1–17, DOI: 10.1002/047084289X.rt247.pub3.
- Examples using triflyl imidazole as a [Tf] source: F. Effenberger and K. E. Mack, *Tetrahedron Lett.*, 1970, **11**, 3947–3948.



- 15 Examples using PhNTf<sub>2</sub> as a [Tf] source: (a) J. B. Hendrickson and R. Bergeron, *Tetrahedron Lett.*, 1973, **14**, 4607–4610; (b) J. E. Mc Murry and W. J. Scott, *Tetrahedron Lett.*, 1983, **24**, 979–982; (c) W. E. Zeller and R. Schwörer, N-Phenyltrifluoromethanesulfonimide, in *Encyclopedia of Reagents for Organic Synthesis*, 2009, DOI: 10.1002/047084289X.rp142.pub2.
- 16 Examples using Comins' reagent as a [Tf] source: D. L. Comins and A. Dehghani, *Tetrahedron Lett.*, 1992, **33**, 6299–6302.
- 17 Apart from phenolic starting materials, aryl triflates have also been made using triflic acid (TfOH) in diazonium or benzyne chemistry, or using metal triflate salts in cross coupling chemistry: (a) O. Planas, V. Peciukenas and J. Cornella, *J. Am. Chem. Soc.*, 2020, **142**, 11382–11387; (b) C. Picherit, F. Wagner and D. Uguen, *Tetrahedron Lett.*, 2004, **45**, 2579–2583; (c) T. Pages and B. R. Langlois, *J. Fluorine Chem.*, 2001, **107**, 321–327; (d) C. Ge, G. Wang, P. Wu and C. Chen, *Org. Lett.*, 2019, **21**, 5010–5014; (e) A. Pialat, B. Liégault and M. Taillefer, *Org. Lett.*, 2013, **15**, 1764–1767.
- 18 T. Gramstad and R. N. Haszeldine, *J. Chem. Soc.*, 1956, 173–180, DOI: 10.1039/JR9560000173.
- 19 Y. Wang, Z. Gao, B. Wang, W. Zhou, P. Yu and Y. Luo, *Ind. Eng. Chem. Res.*, 2019, **58**, 21913–21920.
- 20 (a) L. Conte, G. Gambaretto, G. Caporiccio, F. Alessandrini and S. Passerini, *J. Fluorine Chem.*, 2004, **125**, 243–252; (b) M. Kobayashi, T. Inoguchi, T. Iida, T. Tanioka, H. Kumase and Y. Fukai, *J. Fluorine Chem.*, 2003, **120**, 105–110; (c) T. J. Brice and P. W. Trott, Fluorocarbon Sulfonic Acids and Derivatives, *US Pat.*, US2732398A, 1956.
- 21 T. Kume, T. Morinaka, T. Nanmyo and S. Sakai, Process for Preparation of Trifluoromethanesulfonyl Fluoride, *European Patent*, EP2216325A1, 2010.
- 22 Y. Morino and Y. Tateishi, Method for Producing Trifluoromethanesulfonyl Fluoride, *Japan Patent*, 2008285419A, 2008.
- 23 For applications of CF<sub>3</sub>SO<sub>2</sub>F in synthetic chemistry, see: (a) D. M. Barnes, V. S. Chan, T. B. Dunn, T. S. Franczyk, A. R. Haight and S. Shekhar, Process for Preparing Antiviral Compounds, *US Pat.*, 20130224149A1, 2013; (b) I. Akihisa, U. Koji and Y. Manabu, Method for Producing Acid Fluorides, *Japan Patent*, 2009155248A, 2009; (c) N. Masashi and N. Satoshi, Method for Producing Perfluoroalkanesulfonic Acid Ester, JP2007119355A, 2007; (d) I. Akihiro, U. Mikio, K. Yokusu and T. Mitsuru, Process for Producing Binaphthol Bistriflate, *US Pat.*, 6399806B1, 2002.
- 24 A. Pees, C. Sewing, M. J. W. D. Vosjan, V. Tadino, J. D. M. Herscheid, A. D. Windhorst and D. J. Vugts, *Chem. Commun.*, 2018, **54**, 10179–10182.
- 25 J. Demaerel, C. Veryser and W. M. De Borggraeve, *React. Chem. Eng.*, 2020, **5**, 615–631.
- 26 Y. Zou, L. Qin, X. Ren, Y. Lu, Y. Li and J. Zhou, *Chem. –Eur. J.*, 2013, **19**, 3504–3511.
- 27 D. E. Frantz, D. G. Weaver, J. P. Carey, M. H. Kress and U. H. Dolling, *Org. Lett.*, 2002, **4**, 4717–4718.
- 28 T. Avullala, P. Asgari, Y. Hua, A. Bokka, S. G. Ridlen, K. Yum, H. V. R. Dias and J. Jeon, *ACS Catal.*, 2019, **9**, 402–408.
- 29 A. F. Littke, C. Dai and G. C. Fu, *J. Am. Chem. Soc.*, 2000, **122**, 4020–4028.
- 30 A. S. Voisin-Chiret, A. Bouillon, G. Burzicki, M. Célant, R. Legay, H. El-Kashef and S. Rault, *Tetrahedron*, 2009, **65**, 607–612.
- 31 J. Liu, B. Sun, X. Zhao, J. Xing, Y. Gao, W. Chang, J. Ji, H. Zheng, C. Cui, A. Ji and H. Lou, *J. Med. Chem.*, 2017, **60**, 7166–7185.
- 32 H. Wenschuh, M. Beyermann, E. Krause, M. Brudel, R. Winter, M. Schuemann, L. A. Carpino and M. Bienert, *J. Org. Chem.*, 2002, **59**, 3275–3280.
- 33 R. Y. Garlyauskayte, A. V. Bezudny, C. Michot, M. Armand, Y. L. Yagupolskii and L. M. Yagupolskii, *J. Chem. Soc. Perkin Trans. 1*, 2002, 1887–1889, DOI: 10.1039/B205169A.
- 34 M. Wright, C. Martínez-Lamenca, J. E. Leenaerts, P. E. Brennan, A. A. Trabanco and D. Oehlrich, *J. Org. Chem.*, 2018, **83**, 9510–9516.
- 35 D. D. Liang, D. E. Streefkerk, D. Jordaan, J. Wagemakers, J. Baggerman and H. Zuilhof, *Angew. Chem., Int. Ed.*, 2020, **59**, 7494–7500.
- 36 H. Mukherjee, J. Debreczeni, J. Breed, S. Tentarelli, B. Aquila, J. E. Dowling, A. Whitty and N. P. Grimster, *Org. Biomol. Chem.*, 2017, **15**, 9685–9695.
- 37 J.-N. Luy and R. Tonner, *ACS Omega*, 2020, **5**, 31432–31439.
- 38 A. Laio and M. Parrinello, *Proc. Natl. Acad. Sci. U.S.A.*, 2002, **99**, 12562–12566.
- 39 (a) R. Van Lommel, J. Bock, C. G. Daniliuc, U. Hennecke and F. De Proft, *Chem. Sci.*, 2021, **12**, 7746–7757; (b) G. Bussi and A. Laio, *Nat. Rev. Phys.*, 2020, **2**, 200–212; (c) K. M. Bal, S. Fukuhara, Y. Shibuta and E. C. Neyts, *J. Chem. Phys.*, 2020, 153; (d) R. VanLommel, S. L. C. Moors and F. De Proft, *Chem. –Eur. J.*, 2018, **24**, 7044–7050.
- 40 N-Phenylpiperazine was chosen a higher-MW substrate for the mechanistic experiments because N-triflyl piperidine (the product in the simulations) is volatile and less suited for isolated yield determination.
- 41 (a) J. VandeVondele and J. Hutter, *J. Chem. Phys.*, 2007, **127**, 114105; (b) J. P. Perdew, K. Burke and M. Ernzerhof, *Phys. Rev. Lett.*, 1996, **77**, 3865–3868.
- 42 S. Grimme, J. Antony, S. Ehrlich and H. Krieg, *J. Chem. Phys.*, 2010, **132**, 154104.
- 43 (a) J. Hutter, M. Iannuzzi, F. Schiffmann and J. VandeVondele, *Wires Comput. Mol. Sci.*, 2014, **4**, 15–25; (b) J. VandeVondele, M. Krack, F. Mohamed, M. Parrinello, T. Chassaing and J. Hutter, *Comp. Phys. Commun.*, 2005, **167**, 103–128.
- 44 T. A. Hamlin, M. Swart and F. M. Bickelhaupt, *ChemPhysChem*, 2018, **19**, 1315–1330.
- 45 (a) M. Iazykov, M. Canle, J. A. Santaballa and L. Rublova, *Int. J. Chem. Kinetics*, 2015, **47**, 744–750; (b) S. Yamabe, G. Zeng, W. Guan and S. Sakaki, *J. Comput. Chem.*, 2014, **35**, 1140–1148; (c) T. W. Bentley, R. O. Jones, D. H. Kang and I. S. Koo, *J. Phys. Org. Chem.*, 2009, **22**, 799–806.
- 46 E. R. Johnson, S. Keinan, P. Mori-Sánchez, J. Contreras-García, A. J. Cohen and W. Yang, *J. Am. Chem. Soc.*, 2010, **132**, 6498–6506.

